PROGRESS REPORT FOR SECOND YEAR

For National Aeronautics and Space Administration Proposal:

Development of a Model of Atmospheric Oxygen Variations to Estimate Terrestrial Carbon Storage and Release

ORIGINAL CONTAINS
COLOR ILLUSTRATIONS

First year: 1 January 1993 to 31 December 1993

Second year: 1 May 1994 to 30 April 1995

Raymond G. Najjar
Department of Meteorology
The Pennsylvania State University
University Park, PA

Ralph F. Keeling
Scripps Institution of Oceanography
La Jolla, CA

David J. Erickson III
Atmospheric Chemistry Division
National Center for Atmospheric Research
Boulder, CO

NASA Grant No. NAGW-3929

1 INTRODUCTION

We have completed two years of work towards the development of a model of atmospheric oxygen variations on seasonal to decadal timescales. During the first year we (1) constructed a preliminary monthly-mean climatology of surface ocean oxygen anomalies, (2) began modeling studies to assess the importance of short term variability on the monthly-mean oxygen flux, and (3) conducted preliminary simulations of the annual mean cycle of oxygen in the atmosphere. Details of the first year of work can be found in our first progress report. Most of the second year has been devoted to improving the monthly mean climatology of oxygen in the surface ocean.

2 PROGRESS TO DATE

Acquisition of Updated Oceanographic Data Set

During the first year of work we had been working with the Station Data archives as of June 1991 from the National Oceanographic Data Center (NODC). In March 1994 an updated version of this data set was released by NODC. We acquired these data and have been working with them since. The new data set contains more than 880,00 stations and is approximately 20% larger than the previous release. Upon receiving the data set, a number of preliminary checks were made to assess the overall consistency of the format of the data set. For example, we checked that depths increased monotonically, that the numeric fields never contained non-numeric characters, that the mean ship speed between stations was reasonable, that there were no duplicate stations, etc. We corrected the few errors of this type that we found, eliminating stations in some cases.

Of the remaining stations in the data set 36% contained oxygen data. The distribution of these stations reveals the expected high density of stations in the Northern Hemisphere and in coastal waters (Figure 1) as well as a summertime bias in both hemispheres (Figure 2). Most of the measurements in the data set are from the 1960's and 70's, though the data set spans from 1898 to 1991 (Figure 3).

Calculating the Oxygen Anomaly

Since the oxygen saturation concentration is a function of temperature and salinity, the oxygen anomaly can only be computed when temperature and salinity are measured, as well as oxygen. The units the anomaly were computed in are μmol/kg, since molar- and mass-based units are conservative with respect to temperature, salinity and pressure, while volume-based units are not. Before computing the oxygen anomaly, we therefore needed to convert the oxygen concentration from ml O_2/l seawater (which are the units used by NODC) to μmol O_2/kg seawater. The conversion factor used for oxygen at STP is 0.022392 ml/μmol. To convert from liters to kg we used the equation of state at one atmosphere by Millero and Poisson (1981). Having the oxygen concentration in μmol/kg, the oxygen saturation concentration, which is only a function of temperature and salinity, can now be computed. For the oxygen saturation concentration, the recent formula of Garcia and Gordon (1992) is used.

Cleaning the Data

Much of our efforts have been focussed on ways to eliminate bad or unrepresentative data. We considered the following checks: range check, standard deviation check, cast check, and cruise check.

Range Check. This type of check eliminates any data outside of a specified range. We applied the range checks of Levitus (1982), but found that they eliminated good data. For example, the overwhelming majority of temperature observations removed by this check came from the middepth (~2000 m) waters of the Mediterranean and Red Seas. Also, most of the salinity observations that violated this check came from near surface (~50 m) and middepth (~1500 m) waters of the Mediterranean, Red, Black and Baltic Seas, as well as the Persian Gulf. A large number of violations also occurred in Puget Sound and at river mouths. The remaining few percent of the violations occurred in other coastal areas. Only about 10 violations of the temperature and salinity range checks occurred in open ocean waters. Most likely, the range check was violated in the inland seas because it was not designed properly for considering the unique hydrographic characteristics of these waters. With regard to the oxygen range check, no violations occurred. We conclude that the range check, as designed by Levitus (1982), is not effective, and decided not to use any of the range checks.

Standard Deviation and Cast Checks. The basic idea with the standard deviation check is to eliminate observations in a particular region that are far from the mean in that region. For example, Levitus (1982) applied the following standard deviation check to the NODC station data. First, the means and standard deviations of a given variable were computed in 10° squares at each standard level, regardless of time. Then, data more than 3 to 5 standard deviations from the mean (depending on depth and proximity to land) were eliminated. Levitus (1982) also performed a cast (station) check on the data. If more than 20% of the observations of a particular variable in a station violated the standard deviation check, then all of the observations of that variable in that station were eliminated. The standard deviation and cast checks were applied twice. We applied this check to the temperature, salinity and oxygen data from an earlier version of the NODC station data. We found that many of the data that were eliminated by this check were located very close to latitudes and longitudes that were multiples of 10. In other words, many of the data eliminated came from near the edges of the 10° squares. This means that these data were not really outliers. Rather, they were just too far from the center of the square to be representative of that square. We quantified this effect by applying this analysis to the temperature part of the data set. We found that 36% of the surface temperature data lay within one degree of lines of constant latitude and longitude that are multiples of 10°. This is to be expected, since the area occupied by these regions is 36% of the total surface area of the earth. However, we found that 74% of the data removed by this standard deviation check was within these "border" areas. This confirmed our suspicions that the standard deviation check was not removing true outliers. We chose, therefore, not to apply this standard deviation check.

Cruise Check. A scheme we are currently exploring is to compare individual cruises of unknown quality with cruises of known high quality. Within the latter set are cruises from GEOSECS, TTO, and SAVE. Starting with these cruises (which we located within the NODC Station Data Archives), we will find out where other cruises overlap and see if the oxygen, temperature, and salinity values are reasonably consistent. If they are not, they will be eliminated from the analysis. If they are consistent, they will be retained and added to the list of "good" cruises. The results we present here are based on data that has not been subject to any cleaning procedure.

Mapping the Data

Selecting the spatial and temporal resolution. The main goal is to produce a seasonal climatology of oxygen in the world ocean, focussing on the basin-wide features of the oxygen distribution. Basin scale features are on the order of 1000 km, so we choose approximately 200 km as the horizontal resolution, which is about 2° in latitude (and 2° in longitude at the equator). Most gridded data, apparently for reasons of convenience, are presented in the familiar equal-angle format (that is, with equal increments in latitude and longitude). We feel, as do Rossow and Garder (1984) that it is more appropriate to present and analyze data on an equal-area grid and that the inconvenience of such a grid is minimal. Therefore we choose a grid that is 2° in latitude and variable in longitude, increasing from 2° in longitude at the equator. Such a grid is not exactly equal-area, since we require there to be an integral number of grid boxes, but it is very close to being equal-area. We arbitrarily choose a longitudinal boundary at the Greenwich Meridian. Whether a point is land or ocean was determined using the topographic data set, ETOPO5, which has a spatial resolution of 5 minutes. If a grid box was more than 50% ocean, it was designated as an ocean box. The grid is shown in Figure 4.

The Mapping Procedure. The first step in producing maps is to compute monthly averages of the oxygen anomaly within the grid boxes. The results for January and July in the surface ocean show the fairly sparse distribution of data points on a monthly basis (Figure 5). Nevertheless, a clear seasonal signal is present. The mapping scheme we used is a simple distance-weighted formulation. The value of the oxygen anomaly at any grid point is simply the distance weighted average of all grid points within 1000 km. The weighting function used is from Cressman (1959):

$$w(s) = \frac{s^2 - d^2}{s^2 + d^2}, \qquad s < d$$

$$w(s) = 0, \qquad s > d$$

where s is the distance between the grid point for which the average is being computed and an observation, and d is the radius of influence, which we take to be 1000 km. An average was computed only if there were five or more points within the radius of influence. Also, we did not allow our radius of influence to cross the isthmus of Panama, nor did we allow it to cross the Bering Strait region. Since the data density is not sufficient to interpolate to every grid point with monthly resolution, we did the following. First, from the monthly binned data, we computed a five month running mean of the oxygen anomaly for each grid box. We applied our mapping routine to these 12 arrays of gridded data and were able to estimate a value of the oxygen anomaly at every grid point for all twelve months, except for a very few regions. For these points, we simply filled them in with the zonal mean of the O_2 anomaly for the given month for the particular ocean. We then computed from our monthly binned data a three month running mean for all 12 months. We mapped these data using our distance-weighted averaging scheme. For grid boxes in which the distance weighted scheme could not be used, for lack of data, we filled these grid boxes in with the 5 month running mean. We then applied our mapping procedure to the monthly mean data, filling in the data poor areas with the three month maps. Finally, the twelve monthly maps were smoothed using the Cressman function with a radius of 1000 km. Results for January and July show the strong seasonal cycle of the oxygen anomaly in both hemispheres (Figure 6). The seasonal cycle is stronger in the Northern Hemisphere than in the Southern Hemisphere. This may be partly due to the higher density of data in the Northern Hemisphere.

3 REMAINING WORK

We intend to complete the remaining work outlined in our first progress report. First, we will assess the importance of data sparsity on the amplitude of the annual oxygen cycle using temperature measurements. Having the corrected maps, we will run a simulation of the mean annual cycle of oxygen and estimate the piston velocity over the ocean, including the correction for short-term variability. Having done this, we can then compute the global mean bubble injection, as discussed in our proposal. We then have an estimate for the air-sea oxygen flux at every ocean grid box, for every month of the year. This flux includes the correction for short term variability and the effect of bubble injection.

Knowing the air-sea oxygen flux, oxygen loss due to fossil fuel burning, and the seasonal oxygen flux due to exchange with the terrestrial biosphere, we will then compute the model-predicted interhemispheric gradient in atmospheric oxygen and compare it with observations. The difference between model and observations will be the estimate of terrestrial carbon storage or release.

REFERENCES

Cressman, G. P. 1959. An operational objective analysis system. *Mon. Weather Rev. 87,* 367-374.

Garcia, H. E. and L. I. Gordon. 1992. Oxygen solubility in seawater: Better fitting equations. *Limnol. Oceanogr. 37,* 1307-1312.

Levitus, S. 1982. *Climatological Atlas of the World Ocean, NOAA Prof. Pap. 13,* U.S. Government Printing Office, Washington, D.C.

Millero, F. J. and A. Poisson. 1981. The international one-atmosphere equation of state of seawater. *Deep-Sea Res. 28,* 625-629.

Rossow, W. B. and L. Garder. 1984. Selection of a map grid for data analysis and archival. *J. Climate and Appl. Meteo. 23,* 1253-1257.

FIGURE CAPTIONS

Fig. 1. Distribution of stations within the NODC Station Data archives as of March 1994 which contain observations of oxygen.

Fig. 2. Number of stations containing oxygen plotted versus month of year for three latitude bands: north of 20°N, 20°S to 20°N, and south of 20°S.

Fig. 3. Number of stations containing oxygen plotted versus year.

Fig. 4. Equal-area grid used for binning and mapping oxygen observations. The projection is an interrupted sinusoidal projection, which is also equal-area.

Fig. 5. The binned oxygen anomaly on the equal-area grid for (a) January and (b) July. Red indicates supersaturation and blue indicates undersaturation.

Fig. 6. The mapped oxygen anomaly on the equal-area grid for (a) January and (b) July. Red indicates supersaturation and blue indicates undersaturation. The stippled regions indicate where the three-month default field was used.

Oxygen STATIONS 315154

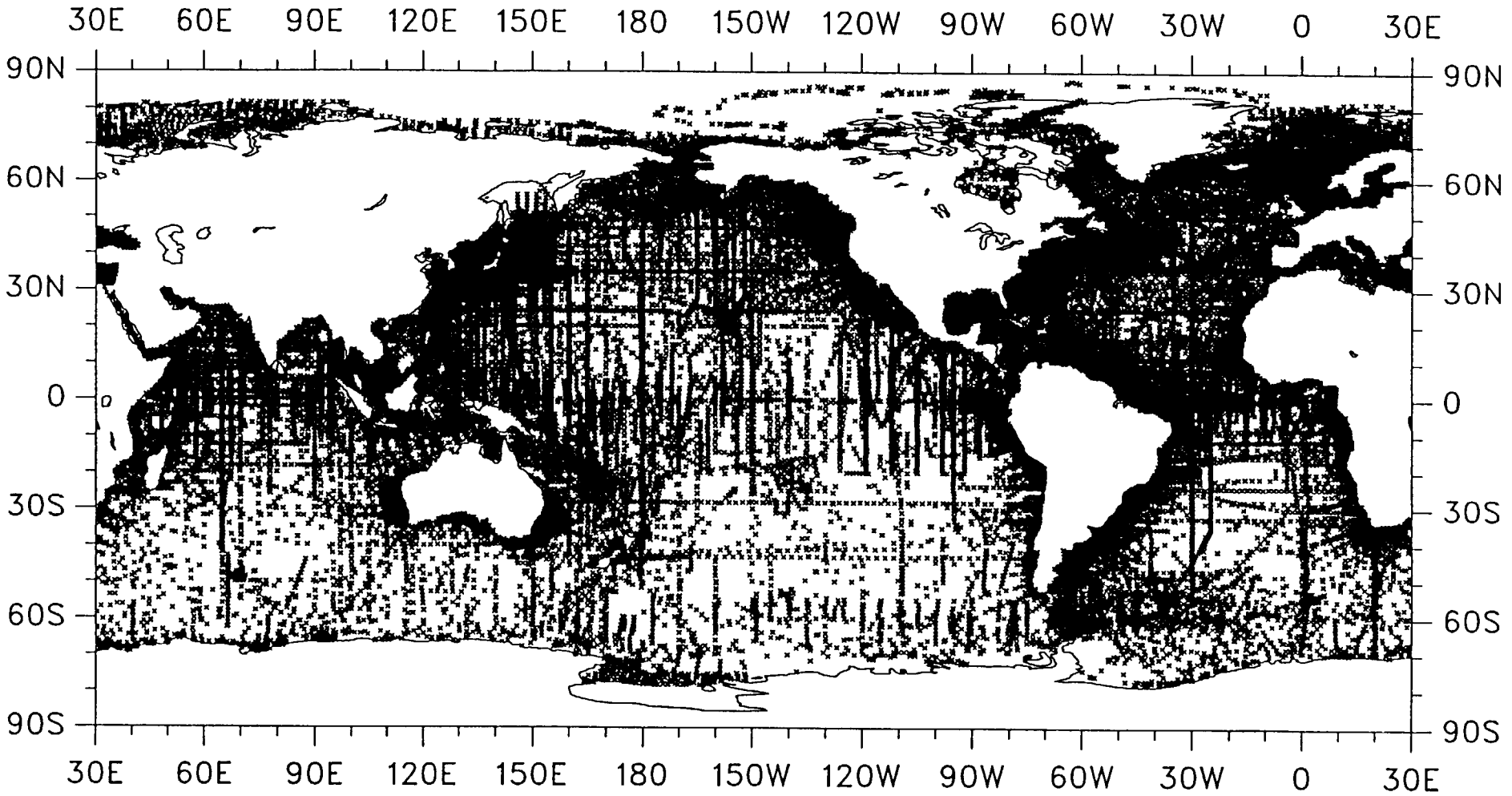

FIGURE 1

FIGURE 2

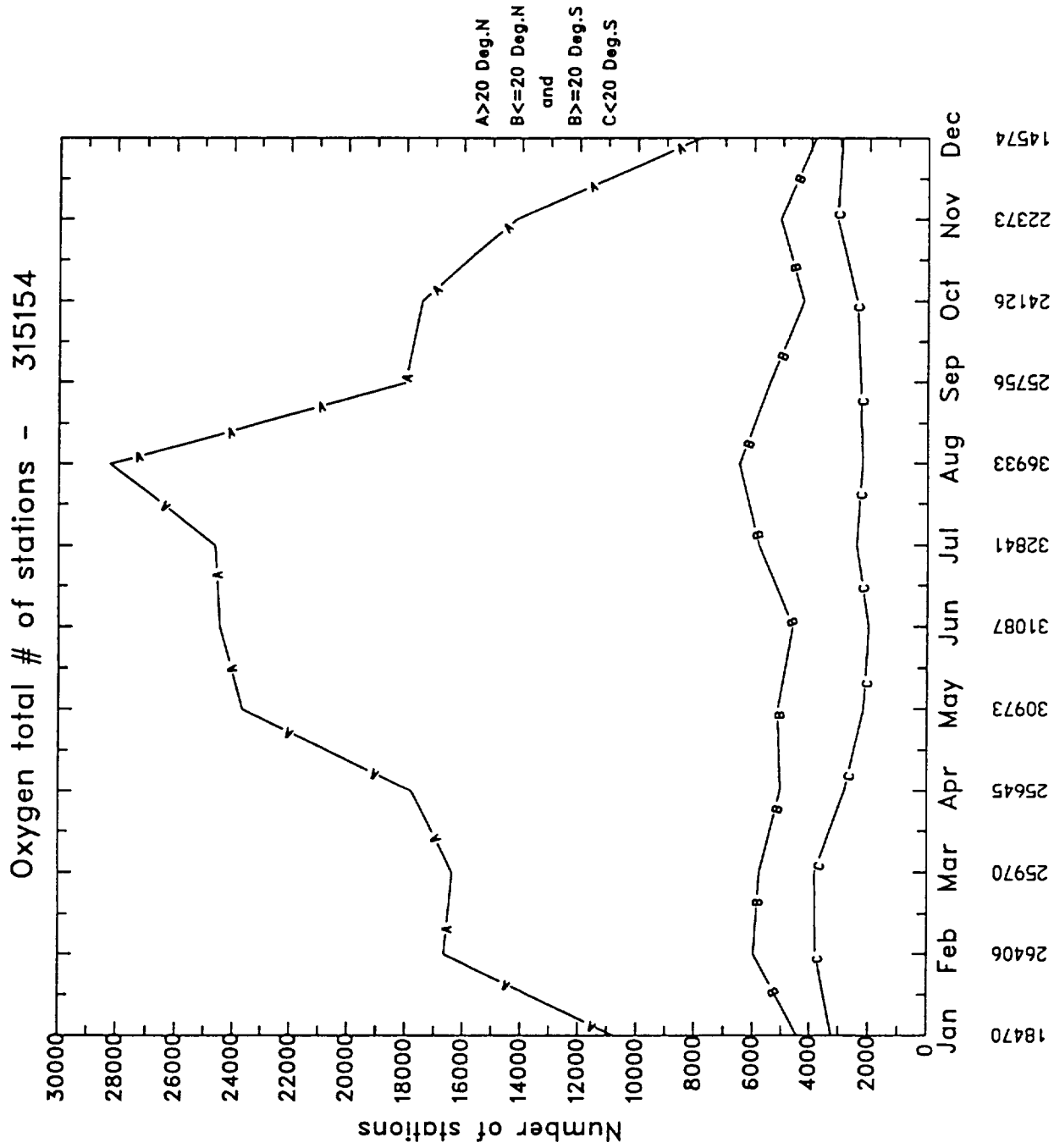
Oxygen total # of stations - 315154
A>20 Deg.N
B<=20 Deg.N
and
B>=20 Deg.S
C<20 Deg.S
Number of stations
0
2000
4000
6000
8000
10000
12000
14000
16000
18000
20000
22000
24000
26000
28000
30000
Jan
Feb
Mar
Apr
May
Jun
Jul
Aug
Sep
Oct
Nov
Dec
18470
26406
25970
25645
30973
31087
32841
36933
25756
24126
22373
14574

FIGURE 3

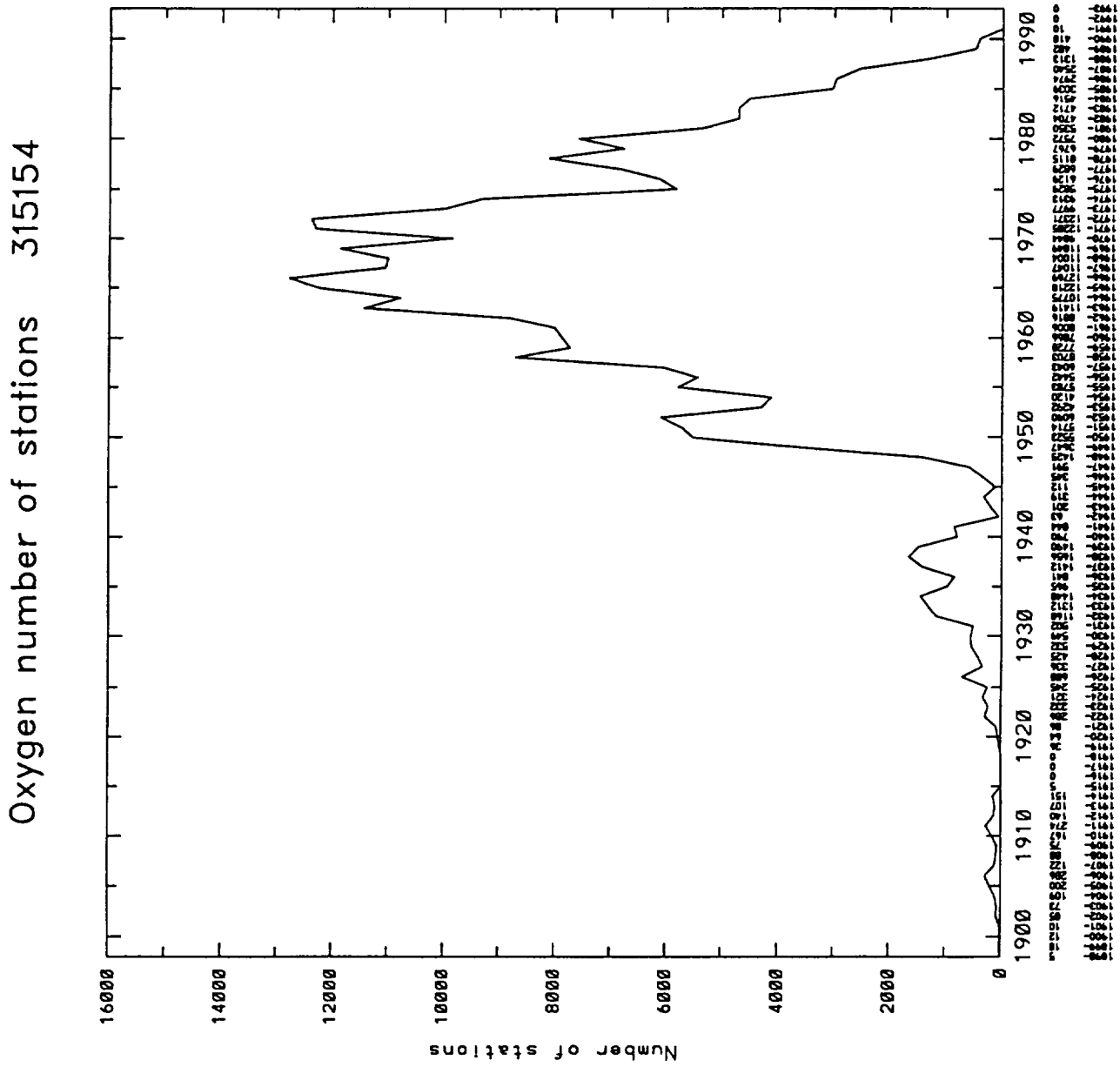
Oxygen number of stations 315154
Number of stations
16000
14000
12000
10000
8000
6000
4000
2000
0
1900
1910
1920
1930
1940
1950
1960
1970
1980
1990

FIGURE 4

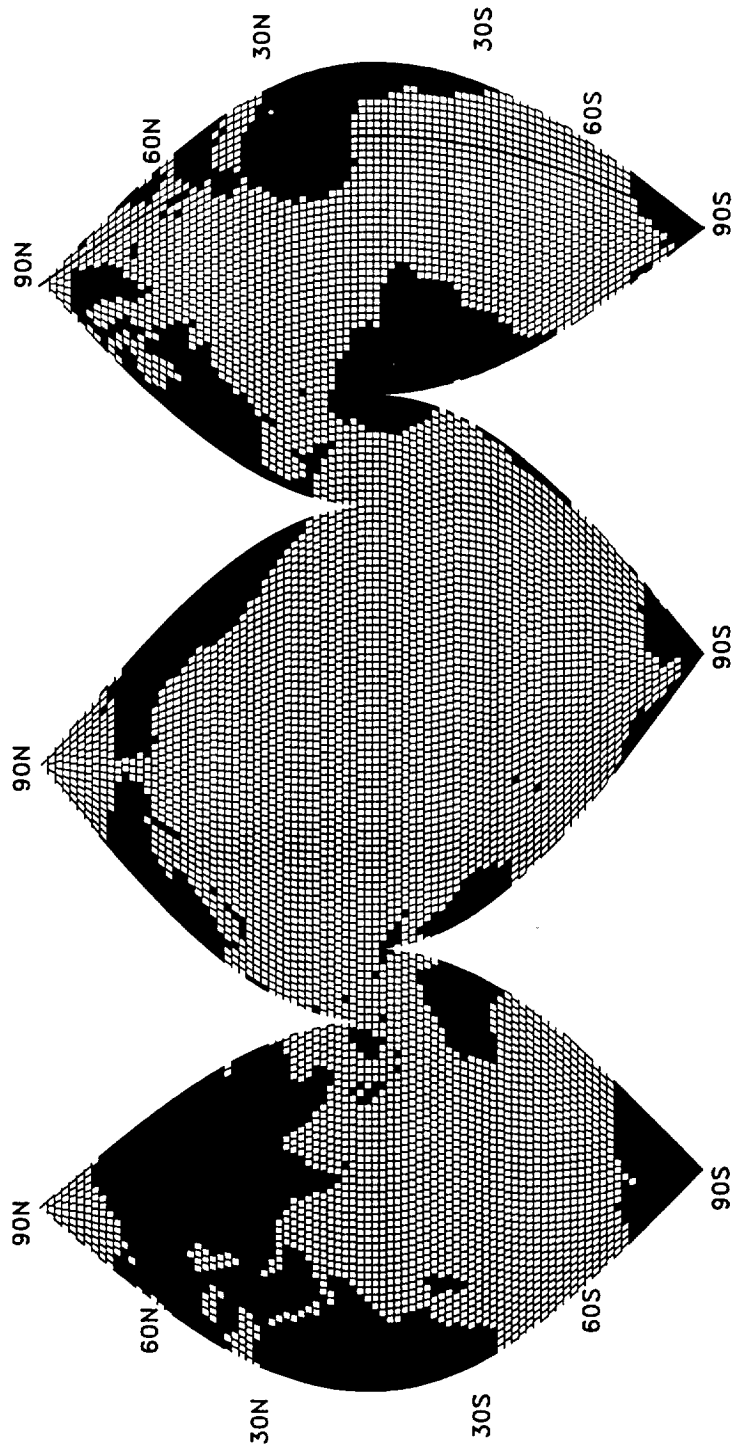

FIGURE 5a

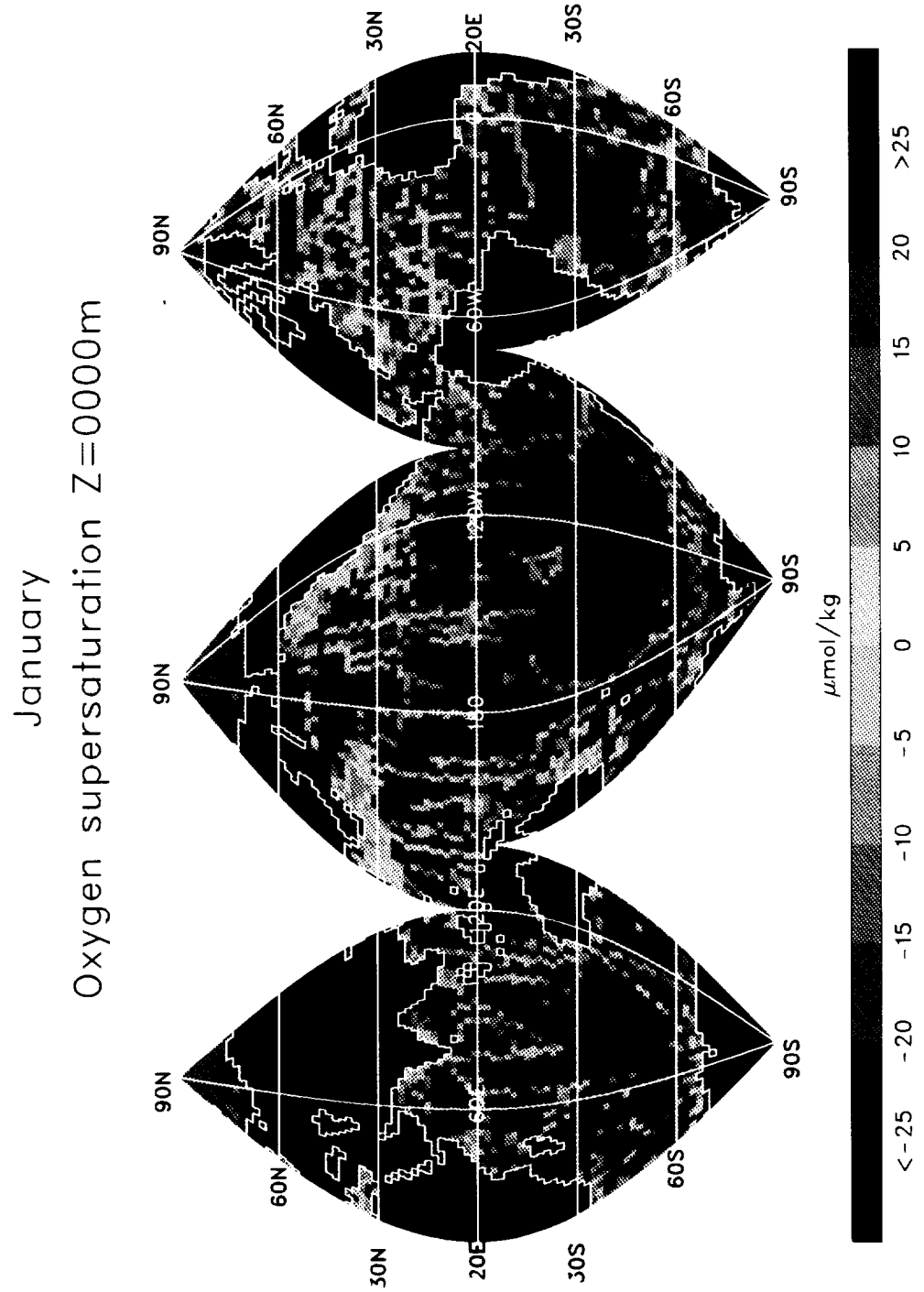
January
Oxygen supersaturation Z=0000m
90N
60N
30N
20E
30S
60S
90S
60W
120W
180
60E
0E
120W
60W
20E
μmol/kg
<-25
-20
-15
-10
-5
0
5
10
15
20
>25

FIGURE 5b

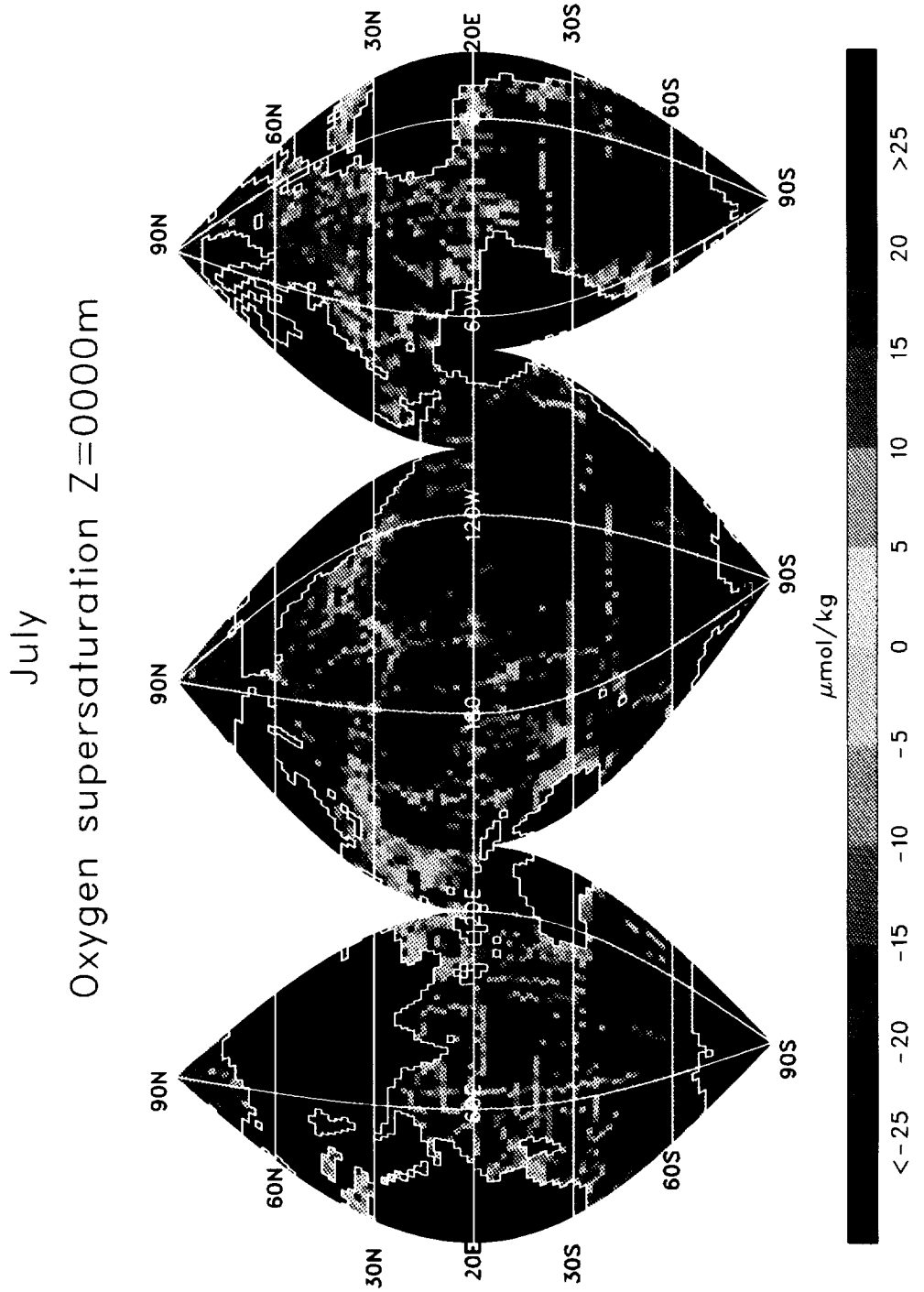
July
Oxygen supersaturation Z=0000m
90N
60N
30N
20E
30S
60S
90S
120W
60W
0
µmol/kg
<-25
-20
-15
-10
-5
0
5
10
15
20
>25

ORIGINAL PAGE
COLOR PHOTOGRAPH

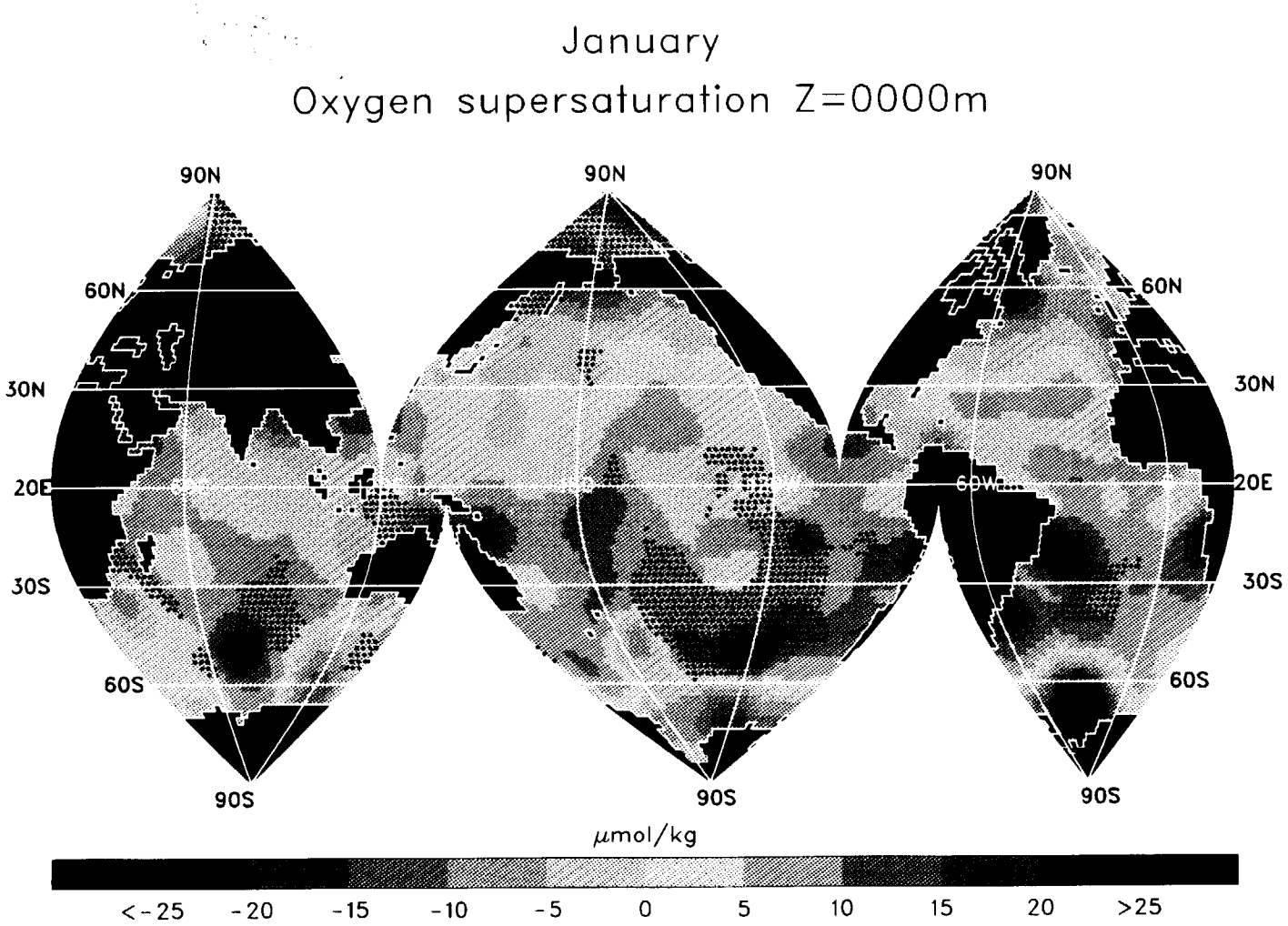

FIGURE 6a

ORIGINAL PAGE
COLOR PHOTOGRAPH

July

Oxygen supersaturation Z=0000m

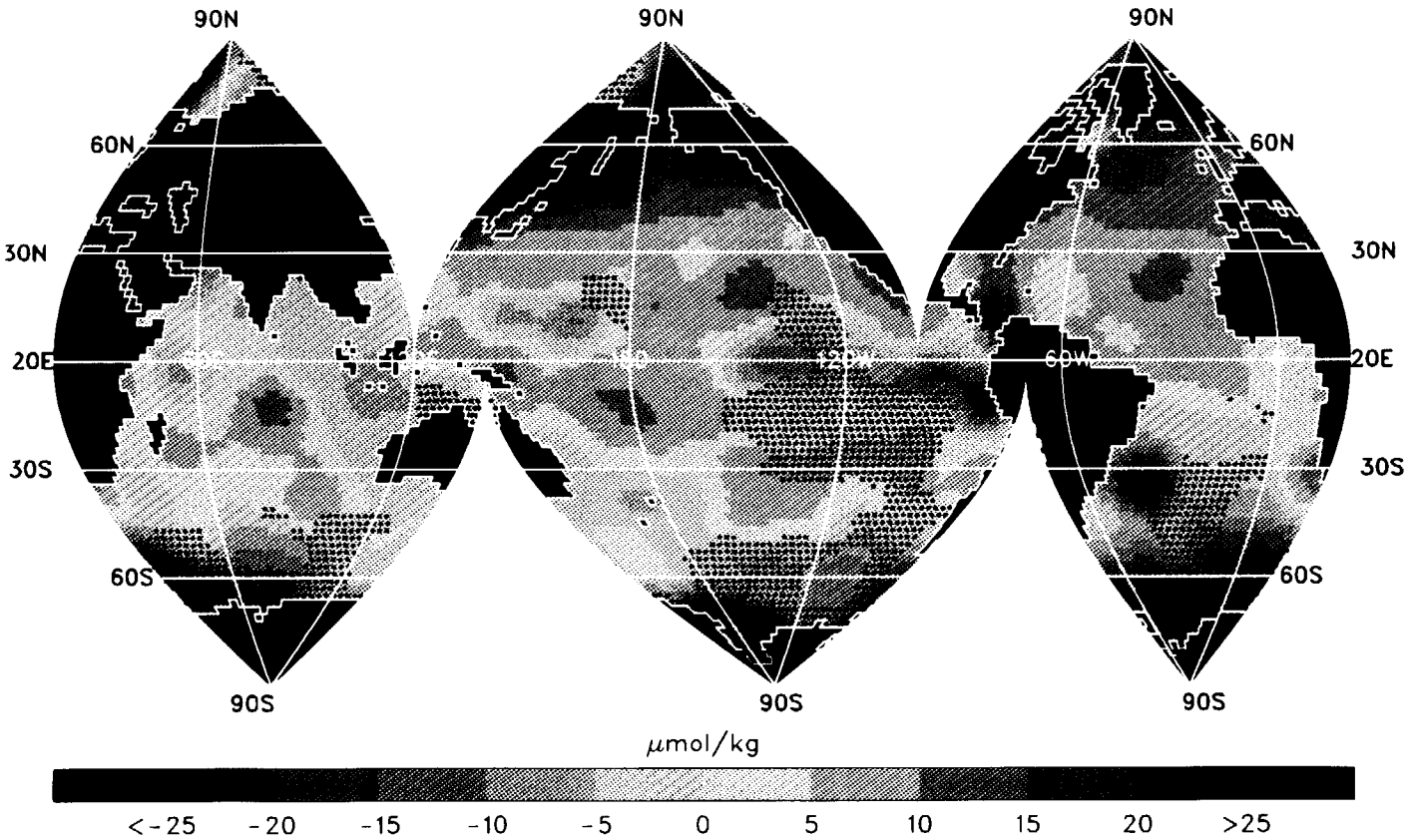

FIGURE 6b